J Am Soc Nephrol 10: 923–934, 1999

Corticosteroid-Dependent Sodium Transport in a Novel Immortalized Mouse Collecting Duct Principal Cell Line

MARCELLE BENS,* VÉRONIQUE VALLET,† FRANÇOISE CLUZEAUD,* LAURENT PASCUAL-LETALLEC,* AXEL KAHN,‡ MARIE E. RAFESTIN-OBLIN,* BERNARD C. ROSSIER,† and ALAIN VANDEWALLE*

**Institut National de la Santé et de la Recherche Médicale (INSERM) Unité 478, Institut Fédératif de Recherche 02, Faculté de Médecine Xavier Bichat, Paris, Cedex, France; †Institut de Pharmacologie et de Toxicologie de l'Université, Lausanne, Switzerland; and ‡INSERM Unité 129, Faculté Cochin, Paris, France.*

Abstract. The final control of sodium balance takes place in the cortical collecting duct (CCD) of the nephron, where corticosteroid hormones regulate sodium reabsorption by acting through mineralocorticoid (MR) and/or glucocorticoid (GR) receptors. A clone of principal CCD cells ($mpkCCD_{cl4}$) has been established that is derived from a transgenic mouse (SV40 large T antigen under the control of the SV40 enhancer/L-type pyruvate kinase promoter). Cells grown on filters form polarized monolayers with high electrical transepithelial resistance (R_T approximately 4700 $\Omega \times cm^2$) and potential difference (P_D approximately -50 mV) and have an amiloride-sensitive electrogenic sodium transport, as assessed by the short-circuit current method (I_{sc} approximately 11 $\mu A/cm^2$). Reverse transcription-PCR experiments using rat MR primers, [^{3}H]aldosterone, and [^{3}H]dexamethasone binding and competition studies indicated that the $mpkCCD_{cl4}$ cells exhibit specific MR and GR. Aldosterone increased I_{sc} in a dose- (10^{-10} to 10^{-6} M) and time-dependent (2 to 72 h) manner, whereas corticosterone only transiently increased I_{sc} (2 to 6 h). Consistent with the expression of 11β-hydroxysteroid dehydrogenase type 2, which metabolizes glucocorticoids to inactive 11-dehydroderivates, carbenoxolone potentiated the corticosterone-stimulated I_{sc}. Aldosterone (5×10^{-7} M)-induced I_{sc} (fourfold) was associated with a three- to fivefold increase in α-ENaC mRNA (but not in those for β- or γ-ENaC) and three- to 10-fold increases in α-ENaC protein synthesis. In conclusion, this new immortalized mammalian CCD clonal cell line has retained a high level of epithelial differentiation and sodium transport stimulated by aldosterone and therefore represents a useful mammalian cell system for identifying the genes controlled by aldosterone.

The distal portions of the renal tubule are the main sites of sodium reabsorption that are regulated by aldosterone (1). Most *in vitro* studies on ion transport regulated by aldosterone or studies on aldosterone-induced proteins and regulation of the amiloride-sensitive sodium channel (ENaC) have been performed on amphibian cell lines (2–5). Aldosterone acts on sodium transport in A6 cells derived from the kidney of *Xenopus laevis* (6) with a latent period (45 min), followed by early (1 to 3 h) and late (3 to 24 h) phases during which sodium transport increases (1,4). These cells form a tight epithelium and bear apical ENaC, which is the rate-limiting step for sodium entry, and a basolateral, ouabain-sensitive sodium pump (Na^+,K^+-ATPase), which provides the driving force for sodium exit (7). Canessa *et al.* (8,9) have determined the primary structure of ENaC from the rat distal colon by expression cloning in *Xenopus laevis* oocytes. ENaC is composed of three homologous subunits (α, β, and γ). The reconstituted channel has the characteristics of the native ENaC described in A6 cells and rat cortical collecting duct (CCD) (10,11) when injected in *Xenopus* oocytes. Immunocytochemical studies on kidneys from rats on a low salt diet have also shown that the three α-, β-, and γ-ENaC subunits are present at the apical membrane of the majority (presumably principal cells) of cortical and outer medullary collecting duct cells (12).

Whether the time course and dose dependence of aldosterone-induced sodium transport in the amphibian A6 cell model are the same as their mammalian counterpart is not known. There is as yet no evidence of a highly conserved response to aldosterone in established mammalian CCD cell lines (13–15). Thus, a mammalian immortalized CCD cell line that responds to aldosterone would be most useful for analyzing the action of corticosteroid hormones on sodium transport.

Targeted oncogenesis in transgenic animals is a powerful method for deriving differentiated renal cell lines (16). We have established differentiated renal proximal tubule and crypt intestinal cell lines (17,18) from transgenic mice carrying the large T antigen gene (Tag) under the control of the 5′ regulatory sequences of the L-type pyruvate kinase (L-PK) gene (19). This transgene is only active in the proximal renal tubule, but an altered expression of integrated transgene was found in another line of transgenic mice (SV-PK/Tag mice) in which the

Received July 8, 1998. Accepted December 3, 1998.
Correspondence to Dr. Alain Vandewalle, Institut National de la Sante et de la Recherche Medicale U478, Faculté de Médecine Xavier Bichat, B.P. 416, 75870 Paris Cedex 18, France. Phone: 33 1 44856326; Fax: 33 1 42291644; E-mail: vandewal@bichat.inserm.fr
1046-6673/1005-0923$03.00/0
Journal of the American Society of Nephrology

large T antigen gene is under the control of the SV40 early enhancer placed in front of the −1004-bp region of the L-PK promoter (20). The large T antigen is detected in proximal tubule cells and also at a high degree in ascending limbs of Henle's loop, distal tubule, and collecting duct cells. This particular strain of SV-PK/Tag transgenic mice was used to derive CCD cells whose chloride transport is sensitive to vasopressin and aldosterone (21). We therefore raised another CCD cell line derived from another SV-PK/Tag transgenic mouse and cloned them to establish a pure population of CCD principal cells, as these are the main target cells for aldosterone in the mammalian kidney (22).

The present study describes the major properties of a clonal cell line, mpkCCD$_{cl4}$, derived from CCD segments isolated from the kidney of a 1-mo-old SV-PK/Tag transgenic mouse. These cells have many of the features expected of an aldosterone-responsive cell when grown on a porous substrate.

Materials and Methods

Materials

Culture media (Dulbecco's modified Eagle's medium [DMEM], Ham's F12) were from Life Technologies (Eragny, France). [α-^{32}P]dCTP and [^{3}H]corticosterone were from New England Nuclear (Le Blanc Mesnil, France). [^{3}H]aldosterone and [^{3}H]dexamethasone were from Amersham (Les Ulis, France). Hormones and reagents were from Sigma (St. Louis, MO). The polyclonal rabbit anti-Tag antibody was a gift from D. Hanahan (University of San Francisco, CA). The anti-cytokeratins K_8-K_{18} antibody was kindly provided by D. Paulin (Université Paris VII, France). The anti-ZO-1 antibody was from Chemicon International (Temecula, CA). The anti-α-Na^+,K^+-ATPase antibody was a gift from M. Caplan (Yale University, New Haven, CT), and the biotinylated *Dolichos biflorus* agglutinin (DBA) was purchased from Vector Laboratories (Burlingame, CA). The RNA-PLUS extraction kit was purchased from Bioprobe Systems (Montreuil-sous-Bois, France). The Moloney murine leukemia virus reverse transcriptase was from Life Technologies. HPLC was performed with the Beckman Gold HPLC system apparatus (Beckman Instruments, Gagny, France). Tissue Culture Treated Transwell or Snapwell filters (0.4 μm pore size, 1.2 cm^2 diameter) were from Corning Costar Corp. (Cambridge, MA). The Millicell Electrical Resistance Clamp apparatus (VCC 600) was from Precision Instrument Design (Tahoe City, CA).

Transgenic Mice

Experiments were carried out on SV-PK/Tag transgenic mice containing a 2.7-kb fragment of the SV40 early region, including the sequences encoding the transforming large tumor (T) and small tumor (t) antigens under the control of the SV40 enhancer placed in front of the −1004 nt fragment of the rat L-L′-pyruvate kinase gene regulatory region in the 5′ flanking region (20).

Cell Isolation and Culture

The kidneys from a 1-mo-old SV-PK/Tag male mouse were removed under sterile conditions, sliced, and incubated in medium (DMEM:Ham's F_{12}, 1:1 vol/vol) containing 0.1% (wt/vol) collagenase for 1 h at 37°C. The slices were rinsed in medium, and CCD fragments were microdissected using sterile fine needles. Pools of five to 10 isolated CCD fragments were rinsed in fresh medium, transferred to collagen-coated 24-well trays, and cultured in modified DM medium (DMEM:Ham's F_{12}, 1:1 vol/vol; 60 nM sodium selenate; 5 μg/ml transferrin; 2 mM glutamine; 50 nM dexamethasone; 1 nM triiodothyronine; 10 ng/ml epidermal growth factor; 5 μg/ml insulin; 20 mM D-glucose; 2% fetal calf serum [FCS]; and 20 mM Hepes, pH 7.4) at 37°C in 5% CO_2/95% air. The cells grew faster after the first passage. They were cloned after the fourth passage and selected for their epithelioid phenotype and the presence of SV40 large T antigen in the nucleus. One clone of cells (mpkCCD$_{cl4}$) was routinely subcultured, and the medium was changed every 2 d. All studies described in this report were performed on cells between the 15th and 40th passages.

Electrophysiologic Studies

Confluent cells seeded and grown in DM medium on collagen-coated Transwell or Snapwell filters were placed in hormone-free, epidermal growth factor-free DM (HFM) medium supplemented with charcoal-treated steroid-free FCS for 24 h, and then in FCS-free HFM medium in which Hepes was replaced by 15 mM $NaHCO_3$ for an additional 18 h. I_{sc} was directly measured using Snapwell filters mounted in a diffusion chamber (Costar Corp.) and connected to a voltage clamp apparatus (VCC 600, Precision Instrument Design) via glass barrel Micro-Reference Ag/AgCl electrodes (Precision Instrument Design) filled with 3 M KCl. Cell layers were bathed on both sides with 8 ml of HFM medium warmed to 37°C and continuously gassed with 95% O_2/5% CO_2 to keep the pH at 7.4. I_{sc} (μA/cm^2) was measured by clamping the open-circuit P_D to 0 mV for 1 s. By convention, a positive I_{sc} is a flow of positive charges from the apical to the basal solution. R_T was calculated from P_D and I_{sc} using Ohm's law. For long-term experiments (≥6 h), transepithelial electrical resistance (R_T) and transepithelial potential (P_D) were measured on cells grown on Transwell filters using dual silver/silver chloride (Ag/AgCl) electrodes connected to the Millicell Electrical Resistance System. Equivalent short-circuit current (I_{eq}) was calculated with Ohm's law from R_T and P_D.

Electron Microscopy

Confluent cells grown on 0.4-μm pore filters were fixed by immersion for 2 h in 2.5% glutaraldehyde in 0.1 M cacodylate buffer, embedded in Epon, and processed for transmission electron microscopy by standard procedures.

Immunohistochemical Methods

The frozen kidneys from an adult SV-PK/Tag transgenic mouse fed a carbohydrate-rich diet and confluent cultured cells were fixed with 60% acetone-30% ethanol, and the SV40 large T antigen was immunolocalized using an anti-Tag polyclonal antibody (20). Confluent cells grown on glass coverslips or porous filters were also fixed in ice-cold methanol for 8 min and processed for immunofluorescence using anti-cytokeratins K_8-K_{18}, anti-ZO-1, anti-α-Na^+,K^+-ATPase antibodies (18,21), or biotinylated *Dolichos biflorus* agglutinin. Specimens were examined under a Zeiss photomicroscope or by confocal laser scanning microscopy (Leica).

Immunoprecipitation Studies

Immunoprecipitation studies were done using preimmune sera and specific anti-α, -β, and -γ rat ENaC (rENaC) antibodies (12) as described by May *et al.* (23). Confluent cells (day 7) grown on porous filters in hormone-free, FCS-free medium were rinsed in methionine-free medium, and 200 μl of methionine-free medium containing 1 mCi/ml [^{35}S]methionine was added to the basal side of inverted filters for 30 min at 37°C. Cells were rinsed again and incubated with 250 μl

of homogenizing buffer (150 mM NaCl, 20 mM Tris-HCl, 5 mM ethylenediaminetetra-acetic acid [EDTA], 1% [vol:vol] Triton X-100, 0.2% bovine serum albumin [BSA], 1 mM phenylmethylsulfonyl fluoride, and 10 μg/ml leupeptin) for 10 min at 4°C. Cells were scraped off, freezed-thawed, sonicated, and centrifuged (15,000 $\times$ *g* for 2 min) to eliminate nuclei and cell debris. The amount of incorporated [^{35}S]methionine was determined by TCA (10%) precipitation. Similar amounts of cpm were submitted to immunoprecipitation. Sodium dodecyl sulfate (SDS; final concentration: 3.7%) was added and samples were heated for 5 min at 95°C. Preparations were precleared with each of the preimmune sera (diluted 1:20) plus 50 μl of pansorbin (0.1 g/ml) for 60 min at 4°C, centrifuged, and then incubated with the specific anti-α, -β, or -γ rENaC antibodies (1:20) overnight at 4°C. Samples were incubated with protein A-Sepharose for 60 min at 4°C, centrifuged, and washed 4 times with the homogenizing buffer and then 3 times with 0.1% SDS, 2 mM EDTA, 10 mM Tris-HCl, pH 7.5. The immunoprecipitated proteins were recovered in Laemmli loading buffer, heated, loaded on 7.5% SDS-polyacrylamide gels, and electrophoresed. Gels were fixed, incubated in Entensify™ solutions (Dupont de Nemours, Brussels, Belgium), and dried. Gels were analyzed with an Instant Imager™ (Hewlett Packard, Meriden, CT) for quantification and then autoradiographed.

cAMP Assay

The influence of deamino-8-D-arginine vasopressin (dDAVP) and isoproterenol (ISO) on the cell cAMP content was assayed as described earlier (21).

RNA Extraction and Reverse Transcription-PCR

Total RNA were extracted from rat and mouse kidneys and confluent mpkCCD$_{cl4}$ cells grown on porous filters using the RNA-PLUS extraction kit. RNA (2 μg) was reverse-transcribed with Moloney murine leukemia virus-reverse transcriptase at 42°C for 45 min. A total of 100 ng cDNA and non-reverse-transcribed RNA from mpkCCD$_{cl4}$ cells was amplified for 25 to 28 cycles in 100 μl of total volume of PCR buffer (50 mM KCl, 20 mM Tris-HCl, pH 8.4) containing 40 μM dNTP; 1.5 mM $MgCl_2$; 1 μCi [α-^{32}P]dCTP; 1 U *Taq* polymerase; 29.2, 31.5, or 29.4 pmol of α-, β-, and γ-rENaC primers, respectively; and 9 pmol of hGAPDH (internal standard) primers. The primers used were the same as those described by Hummler *et al.* (24). The thermal cycling program was 94°C for 30 s, 54°C (α-rENaC) or 53°C (β- and γ-rENaC) for 30 s, and 72°C for 60 s. Amplification products were run on a 4% polyacrylamide gel and autoradiographed.

cDNA (250 ng) from rat or mouse kidneys and cultured cells were amplified for 32 to 34 cycles in a 50-μl total volume of PCR buffer containing 40 μM dNTP, 1.5 mM (for 11β-HSD2) or 3.5 mM (for MR) $MgCl_2$, 1 U *Taq* polymerase, 30 or 29 pmol of mouse 11β-hydroxysteroid dehydrogenase type 2 (m11β-HSD2) primers, or 48 pmol of rat MR (rMR) primers. m11β-HSD2 primers (25) were: sense 5′-TCGCCTGAAGCTGCTGCAGAT-3′ in exon 2 and antisense 5′-TGTCTTGGAGCAGCCAGGCTTG-3′ in exon 4 (30 pmol) or sense 5′-TGACGTGGGACTGTCTCCAGT-3′ in exon 3 and antisense 5′-CTGAGCTGCCAGCAATGCATCGAT-3′ in exon 5 (29 pmol). rMR primers, located near the 3′ end of the rat MR coding region, were the same as those described by Todd-Turla *et al.* (26). To assess the MR PCR products identity, amplified products were digested using *Hin*dIII and *Eco*RI as described (26). The thermal cycling programs were 94°C for 30 s, 60°C (11β-HSD2) or 55°C (MR) for 30 s, and 72°C for 60 s. Amplification products were run on 3.5% agarose gel, then stained with ethidium bromide and photographed.

Corticosteroid Binding Studies

Confluent mpkCCD$_{cl4}$ cells were seeded in 100-mm diameter Petri dishes and grown in charcoal-treated steroid-free medium for 48 h, rinsed three times with 10 ml of ice-cold phosphate-buffered saline, gently scraped off the dishes, collected by centrifugation (150 $\times$ *g* for 10 min), and snap-frozen in liquid nitrogen. TEGW buffer (20 mM Tris-HCl, 1 mM EDTA, 10% glycerol, and 20 mM sodium tungstate, pH 7.4) was added to the frozen cell pellets (3:1 buffer/cell vol). The suspended cells were homogenized with a Teflon glass homogenizer and centrifuged at 105,000 $\times$ *g* for 45 min. Cell cytosol preparations were immediately used for steroid binding assays (27). Protein content of the cytosols was measured by the Bradford method (28), using BSA as standard.

Aliquots of cytosol (25 μl) were incubated with 0.1 to 40 nM [^{3}H]aldosterone or [^{3}H]dexamethasone for 4 h at 4°C. Bound (B) and free (F) hormone were separated using the dextran-charcoal method (27), and B was analyzed as a function of F (29). For competition studies, cytosols were incubated for 4 h at 4°C with [^{3}H]aldosterone alone or with excess ($\times$10 or $\times$100) unlabeled aldosterone, RU26752, or RU486. Bound and free hormones were separated with the dextran-charcoal method.

For sucrose gradient analysis, [^{3}H]aldosterone-labeled cytosol (100 μl) was layered on a 5 to 20% sucrose gradient prepared in TEGW buffer, and the tubes were centrifuged for 2 h at 416,000 $\times$ *g* in a Beckman VTi65.2 rotor. Three-drop fractions were collected by piercing the bottom of each tube and radioactivity was counted. BSA (4.6 S) and aldolase (7.9 S) were external standards.

11β-Hydroxysteroid Dehydrogenase Activity

The conversion of [^{3}H]corticosterone to 11-dehydrocorticosterone mediated by 11β-HSD was determined as described previously (30,31). Briefly, confluent mpkCCD$_{cl4}$ cells grown on Petri dishes were incubated in hormonally free medium for 2 h. Afterward, cells were incubated in this medium (500 μl) supplemented with 2 nM [^{3}H]corticosterone and with or without 10^{-6} M carbenoxolone for 4 h at 37°C. The reaction was stopped by adding 500 μl of cold methanol containing 50 μg/ml unlabeled corticosterone and 11-dehydrocorticosterone. Corticosterone metabolites were separated by HPLC using a reversed-phase column Novapack C18 (4 μm; Waters Associates, Milford, MA) with precolumn (C18, 5 μm; Waters Associates) and isocratic elution (flow rate: 1 ml/min) with methanol/H_2O (50% vol/vol). Ultraviolet detection of unlabeled corticosterone and 11-dehydrocorticosterone was determined at 254 nm, and radioactivity was counted in each collected fraction (30,31).

Statistical Analysis

Results are given as means $\pm$ SEM from *n* experiments. Statistical differences between groups were calculated using *t* test.

Results

Morphologic Features of Principal CCD Cells

Immunolabeling of the SV40 T antigen (Tag) was first analyzed on frozen sections of kidney from an adult SV-PK/Tag transgenic mouse fed a high carbohydrate diet. The transgene construct is shown in Figure 1A. Weak Tag immunostaining was found in the nuclei of proximal tubule cells, and the nuclei from distal and collecting duct cells were also heavily labeled (Figure 1, B and C). Cells from CCD fragments in glucose-enriched medium multiplied rapidly after the first passage. Clones were isolated and subcultured. The mpkCCD$_{cl4}$

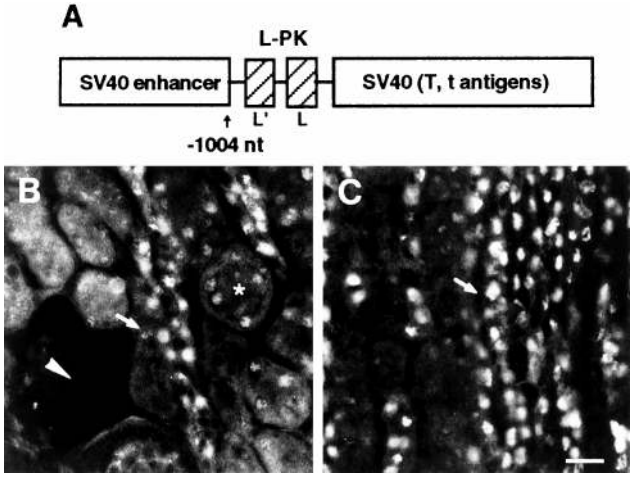

Figure 1. Structure of the SV-PK/T antigen (Tag) construct and Tag expression in the kidney. (A) The SV-PK/Tag construct consists of the 72-bp repeats of the SV40 enhancer from 95 nt to 270 nt inserted into the *Cla*I site (−1004 nt) of the rat L-PK promoter fused to the *Bam*HI-*Bcl*I fragment (2.7 kb) of the SV40 coding sequences of the large tumor (T) and small tumor (t) antigens. Hatched boxes indicate the erythroid- (L′) and liver (L)-specific exons of the L-PK gene. (B and C) Illustrations of the nuclear Tag-positive labeling in tubule cells from kidney cortex (B) and outer medulla (C). Glomeruli are not stained (arrowhead), the nuclei of proximal tubule cells are weakly labeled (asterisk), and nuclei from cortical collecting ducts are heavily labeled (arrows). Bar, 50 μm.

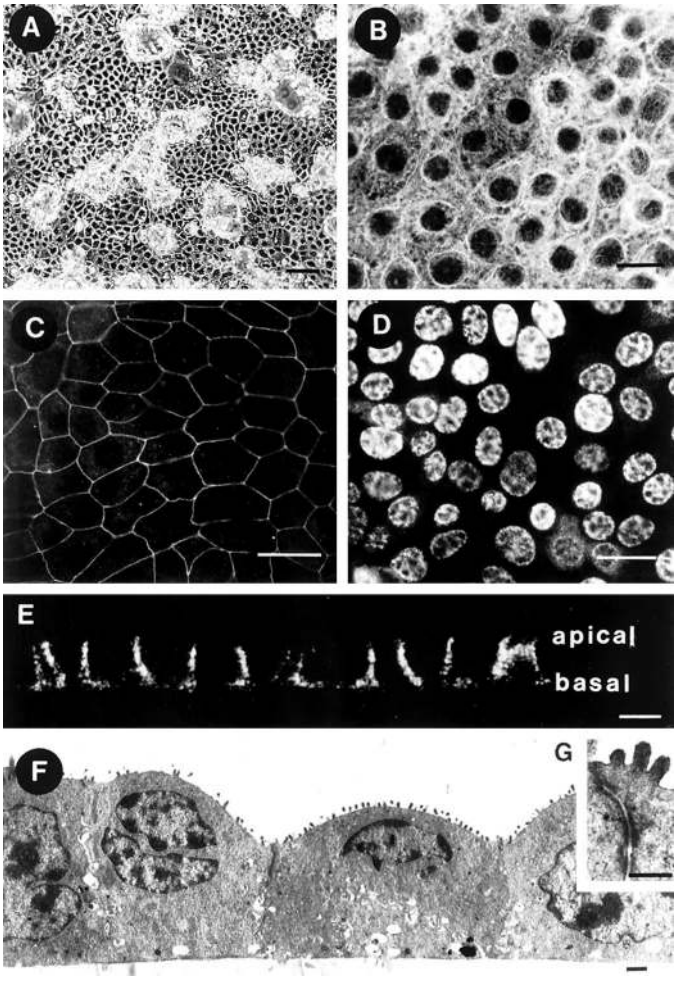

Figure 2. Morphology of confluent cultured mouse cortical collecting duct (CCD) cells. (A) Phase-contrast micrograph of confluent cells grown on a Petri dish (passage 25). The cells are all cuboid and form domes. (B) Cells contain cytokeratins K_8-K_{18}, as detected with a polyclonal antibody. (C) Tight junctions appear as fine, regular outlines around all cells when labeled with the anti-ZO-1 antibody. (D) The nuclei of all cells are immunoreactive for large T antigen. (E) Lateral and basal locations of Na^+,K^+-ATPase pumps is illustrated by confocal laser analysis of preparations labeled with a specific anti-α-Na^+,K^+-ATPase antibody. (F and G) Cells grown on filters form confluent monolayers of closely apposed cuboid cells (F), separated by tight junctions and desmosomes (G). Bars: A, 50 μm; B through E, 10 μm; F and G, 1 μm.

clone was used in the present study. Confluent cells grown on plastic support were all cuboid and formed domes (Figure 2A). Indirect immunofluorescence showed that they contained a typical network of cytokeratins K_8-K_{18} (Figure 2B) and the tight junction-associated protein ZO-1 at the cell peripheries (Figure 2C). The $mpkCCD_{cl4}$ cells grew rapidly (doubling time 20 to 30 h), had a long life span (more than 45 passages to date), and all of their nuclei contained Tag (Figure 2D). Labeling with the anti-α-Na^+,K^+-ATPase antibody analyzed by confocal laser scanning microscopy revealed that Na^+ pumps were in the lateral and basal domains of the cells (Figure 2E). The cells maintained their structural polarity when grown on porous filters and formed monolayers of epithelial cells closely apposed and sealed by typical junctional complexes (Figure 2, F and G).

Biochemical and Functional Properties of Mouse CCD Cultured Cells

Intact CCD contain two cell types, the principal and the intercalated cells, each having distinct sensitivities to hormones and functions (22,32). Deamino-8-D-arginine vasopressin (dDAVP, 10^{-6} M), an analog that binds specifically to the V2 receptors on principal cells, increased the cell cAMP content 43-fold, whereas 10^{-6} M isoproterenol, a β-adrenergic agonist thought to act on intercalated cells (22), increased the cell cAMP only fivefold over that of untreated cells (control: 26 ± 3; dDAVP: 1126 ± 87; ISO: 134 ± 49 pmol/7 min per mg protein; $n = 6$). Immunofluorescence studies with DBA, a lectin that binds to the intercalated cells in the mouse kidney (Figure 3A), showed that very few $mpkCCD_{cl4}$ cells (less than 5%) were DBA-positive (Figure 3, B and C). Hence, the cultured $mpkCCD_{cl4}$ cells were mainly principal cells. These cells also had the typical electrophysiologic features of a tight epithelium; cells grown to confluence on permeable filters developed a high transepithelial electrical resistance (R_T: 4690 ± 234 $\Omega \times cm^2$), a negative potential difference (P_D: −49.1 ± 2.2 mV), and a positive short-circuit current (I_{sc}: +11.1 ± 0.8 $\mu A/cm^2$; $n = 65$).

Reverse transcription (RT)-PCR analyses using specific

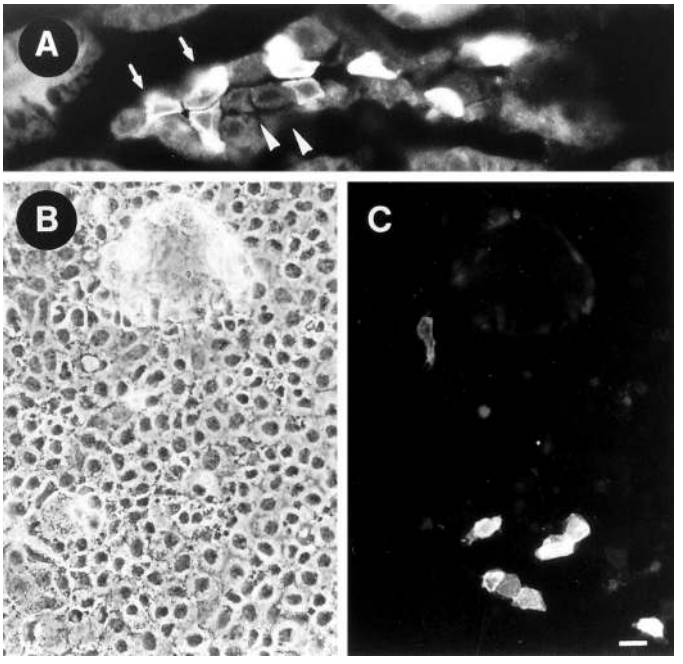

Figure 3. Dolichos biflorus agglutinin (DBA) binding to intact collecting ducts and cultured CCD cells. (A) DBA specifically binds to intercalated cells from intact CCD (arrows), whereas the adjacent pairs of principal cells are not stained (arrowhead). (B and C) Only few cultured $mpkCCD_{cl4}$ cells (less than 5%) are positively stained with DBA, while most of the cells surrounding and forming domes are not stained. Bar, 10 μm.

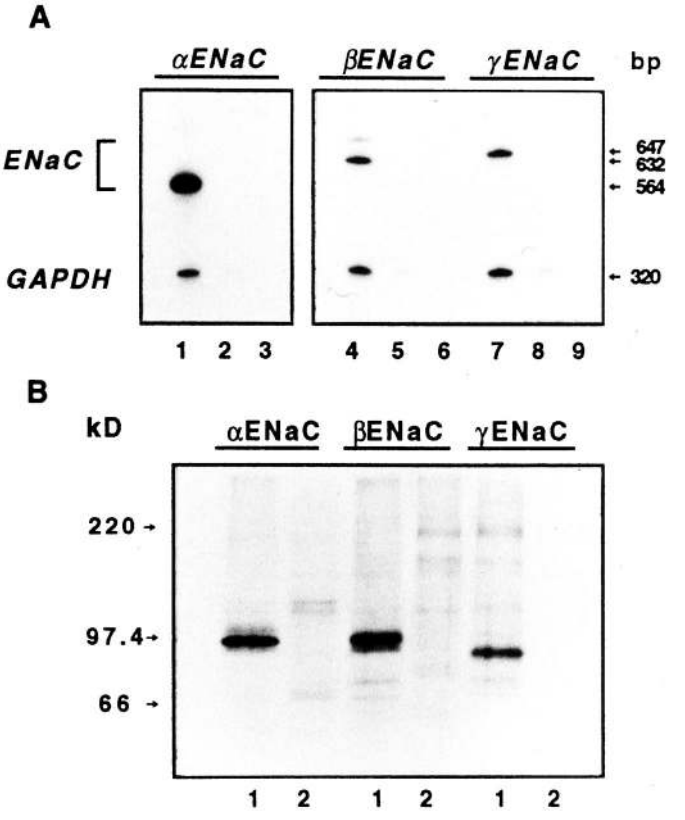

Figure 4. ENaC mRNA and protein in cultured mouse CCD cells. (A) cDNA and non-reverse-transcribed RNA were submitted to reverse transcription (RT)-PCR. Each sample was amplified (28 cycles) with sets of primers specific for α- (lane 1), β- (lane 4), and γ- (lane 7) rENaC and hGAPDH. As control, no amplified products were detected when the mRNA was non-reverse-transcribed (lanes 2, 5, and 8) or when cDNA was omitted (lanes 3, 6, and 9). (B) Proteins were pulsed with [^{35}S]methionine and immunoprecipitated with specific anti-α, -β, and -γENaC sera (lanes 1) and the corresponding preimmune sera (lane 2).

primers indicated that confluent cells grown on porous filters contained mRNA for the three α-, β-, and γ-subunits of the ENaC gene (Figure 4A). There was more α-ENaC mRNA than β and γ mRNA. Immunoprecipitation with rabbit anti-α, anti-β, and anti-γ ENaC sera (23) of cells incubated with labeled methionine revealed heavily ^{35}S-labeled bands of 93 kD for α-ENaC, 96 kD for β-EnaC, and 85 kD for γ-ENaC (Figure 4B). No labeled bands were detected using the corresponding preimmune sera.

Short-circuit current experiments indicated that amiloride added to the apical side of the cells inhibited I_{sc} in a dose-dependent manner (Figure 5A). Benzamyl amiloride, a more potent ENaC channel blocking agent than amiloride (33), also inhibited I_{sc} (Figure 5A). Half-maximum I_{sc} inhibition required 5×10^{-7} M amiloride and 3×10^{-8} M benzamyl amiloride. These Na^+ channel blocking agents had almost no effect on I_{sc} when they were added to the basal side of the filters (Figure 5B). Ethylisopropyl-amiloride, a more specific blocker of the Na^+, H^+ antiport (34), had almost no effect on I_{sc} when it was added to the apical or basal side of the cells (Figure 5, A and B). Ouabain (10^{-4} M) added to the basal side of $mpkCCD_{cl4}$ cells grown on porous filters (not shown) inhibited I_{sc} by $69 \pm 4\%$ ($n = 5$), but did not alter I_{sc} when it was added to the medium bathing the apical side of the cells (data not shown). This is consistent with the detection of the α-subunit of the Na^+,K^+-ATPase in the basolateral membrane of the cells (Figure 2E).

Dose and Time Dependencies of Aldosterone on Stimulated-Sodium Transport

The effect of aldosterone on sodium transport was assessed by measuring I_{sc} on confluent $mpkCCD_{cl4}$ cells grown on filters and incubated in hormone-free, steroid-free medium for 48 h. Aldosterone significantly increased I_{sc} in a dose- and time-dependent manner over that of untreated cells (Figure 6A). All of the aldosterone concentrations tested (10^{-10} M, 10^{-7} M, and 10^{-6} M) increased I_{sc} shortly after 1 h of incubation. Although low, a significant rise in I_{sc} was observed after 2 h of incubation with low aldosterone concentrations ($<10^{-8}$ M) compared with I_{sc} values from the same sets of untreated cells (Figure 6B). The increase in I_{sc} was much more marked for higher concentrations ($>10^{-8}$ M) of aldosterone with maximal increase for 10^{-6} M (Figure 6, A and B).

The stimulatory effect of aldosterone on short-circuit current was maintained over a long period of time. Measurement of the effect of 5×10^{-7} M aldosterone on I_{eq} and R_T of confluent cells grown on porous filters showed that I_{eq} increased soon after 75 min of hormone addition, and the maximal increase

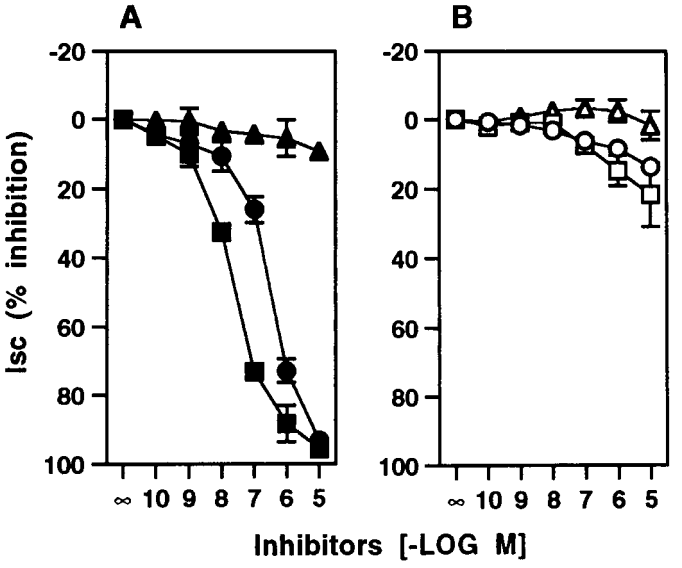

Figure 5. Effects of ENaC blocking agents on I_{sc}. I_{sc} was measured on confluent mpkCCD$_{cl4}$ cells before and after adding amiloride (●, ○), benzamyl amiloride (■, □), or ethylisopropyl-amiloride (▲, △) to the apical side (A) or basal side (B) of the filters for 10 min. Values, expressed as percentage of inhibition of I_{sc} measured before the addition of the blocking agents, are the mean ± SEM from six separate experiments.

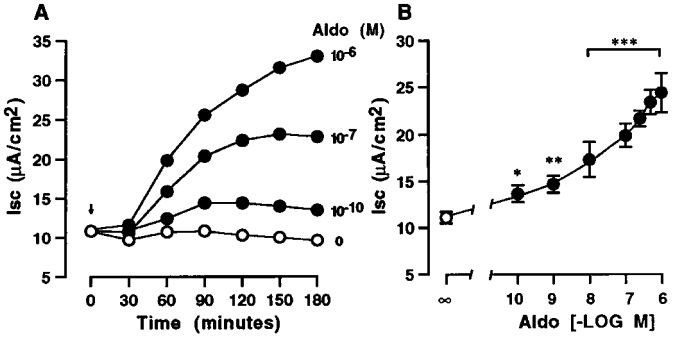

Figure 6. Action of aldosterone on I_{sc}. (A) Representative traces of I_{sc} measured in the absence (○) or presence of 10^{-10}, 10^{-7}, or 10^{-6} M aldosterone (●). (B) Dose-dependent response of I_{sc} after 2 h of incubation with (●) or without (○) various concentrations of aldosterone. Values are means ± SEM of four to seven experiments. *$P <$ 0.05, **$P < 0.01$, ***$P < 0.001$ *versus* untreated cell values (○).

(fourfold) occurred at 6 h and continued for up to 8 h (Figure 7A). I_{eq} slightly decreased thereafter, but was still 4.5-fold higher than in untreated cells after 72 h (control: 7.5 ± 0.3; + aldosterone: 34.1 ± 0.4 μA/cm^2, $n = 3$, $P < 0.001$) when the FCS-free HFM medium was changed daily. The increase in I_{eq} was associated with a significantly large decrease in R_T (Figure 7B). The increase in I_{eq} was due to increased sodium absorption, since I_{eq} was almost completely inhibited by adding 10^{-6} M benzamyl amiloride to the apical side of the cells (Figure 7A, inset). Thus, aldosterone stimulates sodium transport through the amiloride-sensitive epithelial sodium channel.

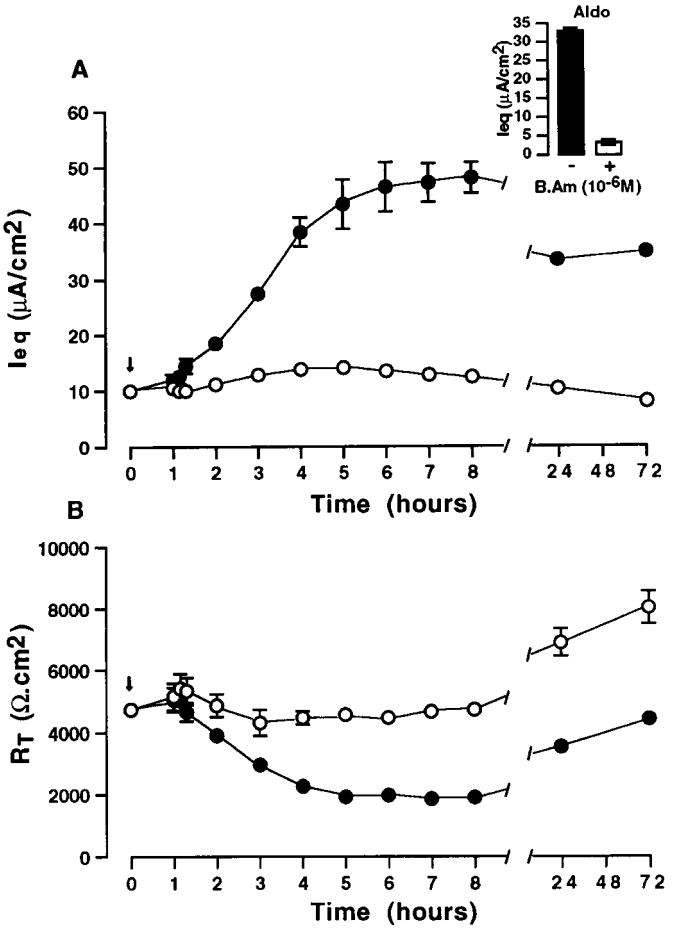

Figure 7. Effect of aldosterone on I_{sc} and R_T. (A) I_{eq} was measured on confluent mpkCCD$_{cl4}$ cells incubated without (○) or with (●) 5×10^{-7} M aldosterone, added (arrows) to both basal and apical sides of the filters for various times. (Inset) Bars represent the mean values ± SEM ($n = 4$) from the 24-h aldosterone-treated cells in the absence (−) or presence (+) of apical benzamyl amiloride (B.Am). (B) R_T was measured on the same sets of filters incubated without (○) or with (●) aldosterone. Values are means ± SEM from six to eight individual filters from eight passages (18th to 30th passages).

Effects of Corticosterone and Carbenoxolone on Sodium Transport: Identification of 11β-HSD2

Previous studies have suggested that glucocorticoids can have mineralocorticoid-like effects on the transport of sodium by primary cultures of rabbit CCD (35) and A6 cells (36,37). The stimulation of sodium transport by corticosterone, the natural glucocorticoid hormone in the mouse, was tested under the same conditions used to study the action of aldosterone. The I_{eq} of mpkCCD$_{cl4}$ cells incubated with 5×10^{-7} M corticosterone for up to 12 h was stimulated (threefold) in the first 2 to 4 h (Figure 8A). The effect of corticosterone was almost completely blocked by adding 10^{-6} M benzamyl amiloride to the apical medium (data not shown). The stimulatory effect of corticosterone gradually decreased after 4 h (Figure 8A). Carbenoxolone (CBX), a potent inhibitor of 11β-HSD (38,39), restored the I_{eq} of cells incubated with corticosterone (5×10^{-7} M) to that of aldosterone-treated cells after 12 h

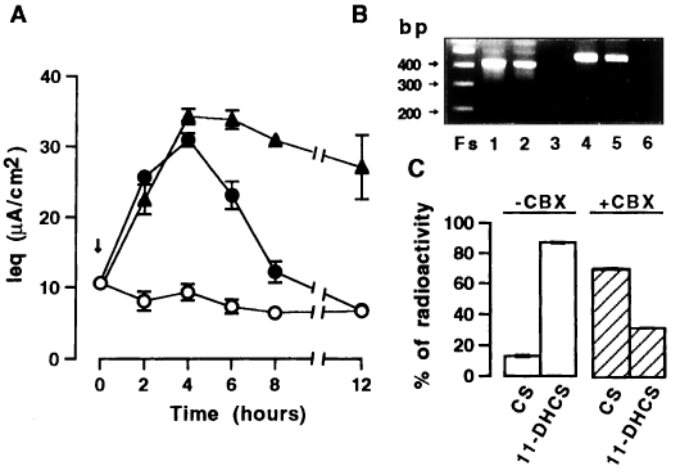

Figure 8. Effects of carbenoxolone (CBX) on corticosterone-stimulated I_{eq} and identification of 11β-HSD2 in cultured mouse CCD cells. (A) I_{eq} was measured on sets of confluent mpkCCD$_{cl4}$ cells grown on filters in the absence (○) or presence (●) of 5×10^{-7} M corticosterone and corticosterone plus 10^{-6} M carbenoxolone (▲) for various times. Corticosterone and carbenoxolone were added (arrow) to the apical and basal side of filters. Values are means ± SEM from six to eight individual filters from eight passages (20th to 35th passages). (B) Samples of cDNA (250 ng) from mouse kidney and cultured mpkCCD$_{cl4}$ cells were amplified by PCR for 32 cycles using primers from m11β-HSD2 exon 2 and 4 (lanes 1 to 3) or exon 3 and 5 (lanes 4 to 6). Amplified products of expected sizes (412 bp: lanes 1 and 2; 475 bp: lanes 4 and 5) were obtained in both mouse kidney (lanes 1 and 4) and cultured CCD cells (lanes 2 and 5). As control, no amplified products were detected by omitting cDNA (lanes 3 and 6). Fs, fragment sizes of DNA molecular weight markers. (C) The conversion, expressed in percentage of total radioactivity, of 2 nM corticosterone (CS) to 11-dehydrocorticosterone (11-DHCS) was measured on confluent mpkCCD$_{cl4}$ cells incubated with 2 nM [^{3}H]corticosterone for 4 h at 37°C in the absence (□) or presence (▨) of 10^{-6} M CBX. Values are means ± SEM of four experiments.

(corticosterone: 6.8 ± 0.3; corticosterone plus CBX: 27.1 ± 4.5; aldosterone: 25.5 ± 0.6 μA/cm^2; $n = 5$). These results suggested that corticosterone was metabolized to inactive metabolites (11-dehydrocorticosterone) by 11β-HSD2, which prevents the illicit occupation of MR by glucocorticoids (40,41). Consistent with these results, 11β-HSD2 mRNA expression was found in mpkCCD$_{cl4}$ cells. RT-PCR experiments performed with two different sets of m11β-HSD2 primers (25) evidenced amplified products of expected size in both mouse kidney and cultured CCD cells (Figure 8B). Furthermore, mpkCCD$_{cl4}$ cells converted corticosterone to 11-dehydrocorticosterone by 87 ± 0.5% ($n = 4$) after 4 h of incubation with 2 nM [^{3}H]corticosterone at 37°C, whereas 10^{-6} M CBX prevented the conversion of corticosterone to 11-dehydrocorticosterone (Figure 8C).

Mineralocorticoid versus Glucocorticoid Receptor Specificity: Physiologic and Pharmacologic Evidence for their Relative Roles in Sodium Transport

Kidney CCD, like other targets for corticosteroid hormones, possess two types of corticosteroid receptors: a high affinity receptor for aldosterone (MR), and a low affinity for aldosterone (GR) (42,43). Aldosterone and corticosterone (or cortisol) bind equally well to both GR and MR. The question therefore is whether the increased sodium absorption elicited by aldosterone was mediated via the occupancy of MR and/or GR. The effects of aldosterone (10^{-9} M and 5×10^{-7} M) and corticosterone (5×10^{-7} M) on I_{sc} were measured with and without excess of RU486, a potent glucocorticoid receptor antagonist in human and rabbit kidneys (Table 1). At all concentrations tested, aldosterone and corticosterone stimulated I_{sc} after 2 h. A 20-fold excess of RU486 prevented the rise in I_{sc} induced by high concentrations of corticosterone or aldosterone, but did not impair the rise in I_{sc} caused by 10^{-9} M aldosterone (Table 1).

Results from RT-PCR experiments using sets of primers located near the end of the rMR 3′ coding region (26) evidenced MR PCR products of expected size (380 bp) in both rat and mouse kidneys (Figure 9A). An additional band was also detected with mouse kidney cDNA. These two amplified products were also detected in mpkCCD$_{cl4}$ cells (Figure 9A). Digestion of the amplified products from whole mouse kidney and cultured cells by *Hin*dIII yielded two bands of 263 and 117 bp long (Figure 9B), as described previously (26). Similarly to that reported for rat kidney (26), two bands (305 and 75 bp) were also obtained by digestion of the amplified products from whole mouse kidney and cultured CCD cells with *Eco*RI (data not shown). These results strongly suggested that cultured mpkCCD$_{cl4}$ cells have retained specific MR mRNA expression.

Steroid binding studies at equilibrium confirmed the presence of MR and GR (Figure 9, C and D). An interaction model with one class of specific and nonspecific binding sites (29) showed that cultured mouse CCD cells had one class of high affinity receptor for aldosterone (K_d: 0.6 nM; N_{max}: 20 to 50 fmol/mg protein) (Figure 9C). No binding of [^{3}H]aldosterone

Table 1. Effects of RU486 on aldosterone- and corticosterone-stimulated I_{sc}[a]

Group	I_{sc} (μA/cm^2)	
	−RU486	+RU486
None	8.7 ± 1.5	7.6 ± 1.2
Aldosterone (10^{-9} M)	15.6 ± 1.5[b]	15.2 ± 2.2
Aldosterone (5×10^{-7} M)	22.8 ± 1.3[c]	11.5 ± 1.3[d]
Corticosterone (5×10^{-7} M)	23.8 ± 1.4[c]	13.1 ± 0.6[d]

[a] I_{sc} was measured on confluent mpkCCD$_{c14}$ cells grown on filters and incubated without (none) or with RU486 (10^{-6} M) or with aldosterone (10^{-9} M and 5×10^{-7} M), aldosterone plus a 20-fold excess of RU486, corticosterone (5×10^{-7} M) and corticosterone plus a 20-fold excess of RU486 for 2 h at 37°C. All hormones and compounds were added to both basal and apical sides of the filters. Values are means ± SEM from three to seven experiments.

[b] $P < 0.05$ *versus* untreated cells.

[c] $P < 0.001$ *versus* untreated cells.

[d] $P < 0.001$ *versus* aldosterone- or corticosterone-treated cells.

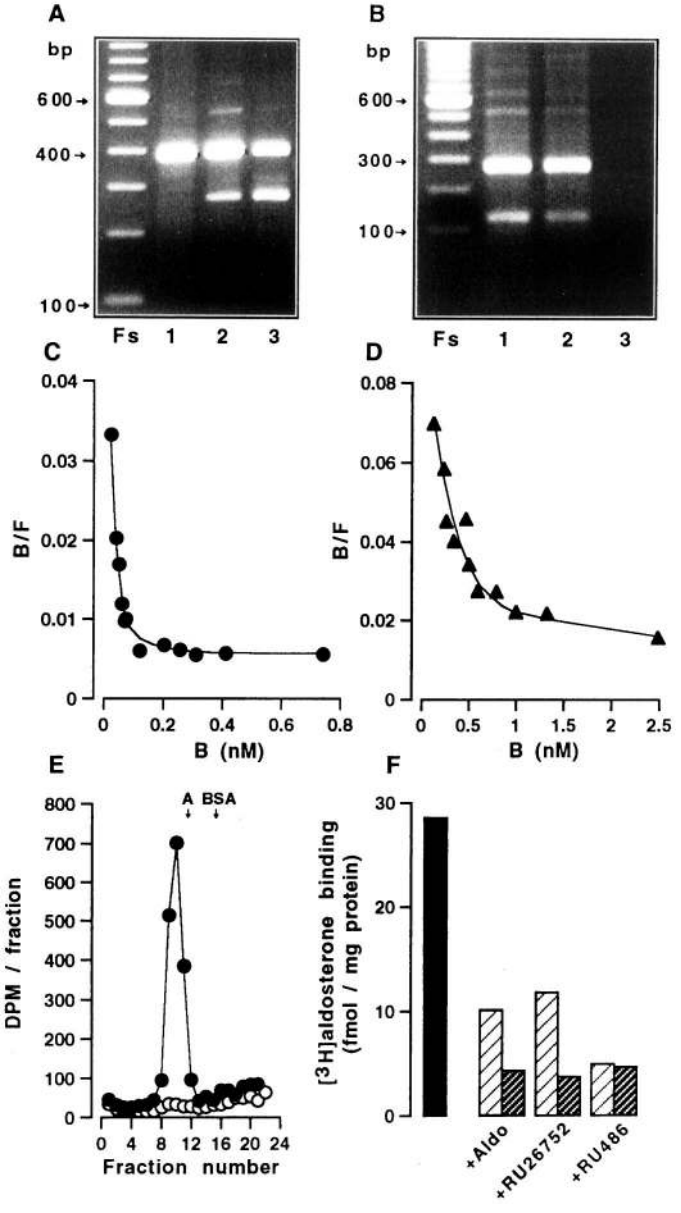

Figure 9. Mineralocorticoid and glucocorticoid receptors in mouse cultured CCD cells. (A) Samples of cDNA (250 ng) from rat and mouse kidneys and cultured mpkCCD$_{cl4}$ cells were amplified by PCR for 34 cycles using sets of rMR primers. Amplified products of the expected size (380 bp) were obtained in rat kidney (lane 1), mouse kidney (lane 2), and cultured CCD cells (lane 3). An additional band of amplified products (not identified) was also detected in mouse kidney and cultured cells. (B) Digestion of the amplified products with *Hin*dIII yielded two bands of expected size (263 bp and 117 bp) in both mouse kidney (lane 1) and cultured CCD cells (lane 2). As control, no amplified products were detected by omitting cDNA (lane 3). Fs, fragment sizes of DNA molecular weight markers. (C and D) Scatchard plots of [^{3}H]aldosterone (●) and [^{3}H]dexamethasone (▲) binding to mpkCCD$_{cl4}$ cytosol. The cytosol was incubated with 0.1 to 40 nM [^{3}H]aldosterone or [^{3}H]dexamethasone for 4 h at 4°C. Bound (B) and free (F) hormone fractions were separated by the dextran-charcoal method. The curve was simulated from the best interaction model, which was one class of specific sites and nonspecific binding. (E) Gradient sedimentation analysis of [^{3}H]aldosterone-receptor complex in the cytosol of mpkCCD cells. Cytosol was incubated with 10^{-8} M [^{3}H]aldosterone for 4 h at 4°C in the absence (●) or presence (○) of a 100-fold excess unlabeled aldosterone. Sedimentation markers were aldolase (A, 7.9 S) and bovine serum albumin (BSA, 4.6 S). (F) The cytosol was also incubated with 10^{-8} M [^{3}H]aldosterone without (black bar) or with a 10-fold (hatched white bars) or 100-fold (hatched black bars) excess of unlabeled aldosterone, RU26752, or RU486.

to GR was detected; however, GR were evidenced by equilibrium binding studies using [^{3}H]dexamethasone as ligand (K_d: 6 nM; N_{max}: 80 fmol/mg protein) (Figure 9D). Sucrose gradient analysis also showed that the peak of [^{3}H]aldosterone-receptor complex sedimented at 8.7 S and appeared to be specific, since it was completely displaced by a 100-fold excess of unlabeled aldosterone (Figure 9E). Competition experiments also showed that the [^{3}H]aldosterone binding was specifically displaced by a 10- and 100-fold excess of both unlabeled aldosterone and RU26752, which has antimineralocorticoid effects because of its affinity for MR *in vivo* and *in vitro* (44,45) (Figure 9F). The specific [^{3}H]aldosterone binding was also displaced by excess RU486, which is consistent with binding of aldosterone to GR (Figure 9E).

ENaC as Mediator of the Amiloride-Sensitive Electrogenic Sodium Transport: Early and Late Effects of Aldosterone

The mpkCCD$_{cl4}$ cells grown on porous filters contain the mRNA-encoding amiloride-sensitive ENaC subunit and the proteins themselves (Figure 4). The effects of aldosterone on the amounts of ENaC mRNA and protein were assessed by growing mouse CCD cells on filters in steroid-free medium for 48 h, then incubating them with 5×10^{-7} M aldosterone (Figure 10). The amounts of α-ENaC mRNA, normalized to the amount of GAPDH mRNA, increased twofold after incubation with aldosterone for 2 h. Longer incubation with aldosterone (6 to 24 h) further increased (three- to fivefold) the amount of α-ENaC mRNA (Figure 10A). In contrast, the amounts of β- and γ-ENaC mRNA did not change (Figure 10A). The rate of α-ENaC protein synthesis also increased threefold after a 2-h incubation with aldosterone (Figure 10B). The increase in α-ENaC protein synthesis remained 10-fold higher after 6 h and sevenfold higher after 24 h of incubation with aldosterone compared with untreated cells (Figure 10B). In contrast, aldosterone did not alter the rate of β-ENaC or the rate of γ-ENaC protein synthesis.

Actinomycin D (a transcription inhibitor) and cycloheximide (a translation blocker) both prevented any increase in I_{eq} by aldosterone (Figure 11A). Immunoprecipitation studies showed that actinomycin D prevented the increase in α-ENaC protein synthesis caused by 2- and 6-h aldosterone treatment (Figure 11B). These data thus provide pharmacologic evidence that the early effect of aldosterone on α-ENaC synthesis requires gene transcription.

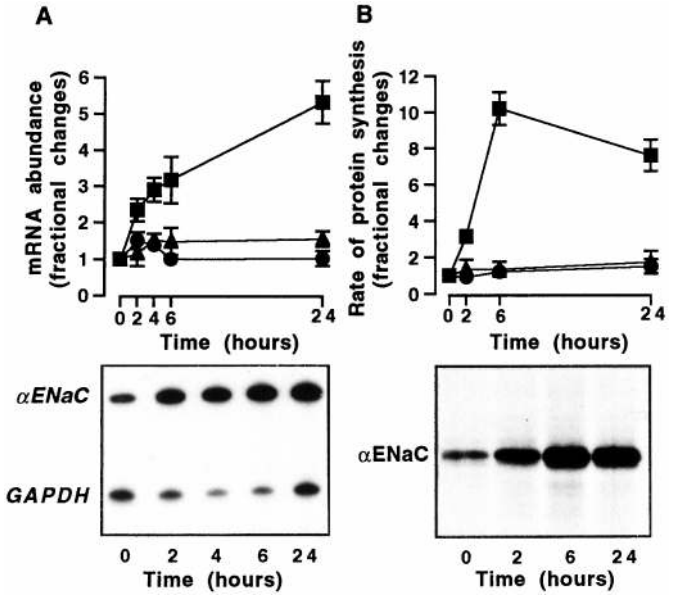

Figure 10. Action of aldosterone on the amounts of ENaC subunit mRNA and protein in cultured mouse CCD cells. Confluent $mpkCCD_{cl4}$ cells grown on filters were incubated without (time 0) or with 5×10^{-7} M aldosterone for 2 to 24 h. (A, Top Panel) cDNA from cells were submitted to RT-PCR and amplified with sets of primers specific for α- (■), β- (●), and γ- (▲) ENaC and GAPDH, used as internal standard. The graph provides the fractional changes in ENaC subunits over GAPDH mRNA ratios (arbitrary unit), which were normalized to 1 for the untreated cells. (A, Bottom Panel) Illustration of time-dependent increase in α-ENaC mRNA expression induced by aldosterone. (B, Top Panel) Rates of α- (■), β- (●), and γ- (▲) ENaC protein syntheses assessed by immunoprecipitation studies. The graph shows the fractional changes in ENaC subunits, normalized to 1 for the values from untreated cells. (B, Bottom Panel) Illustration of the aldosterone-dependent increase in α-ENAC protein synthesis over time. Values are means ± SEM from four separate experiments.

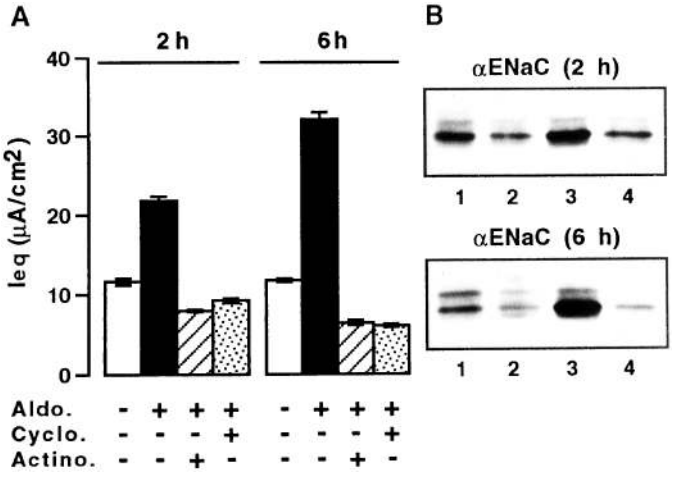

Figure 11. Action of actinomycin D and cycloheximide on aldosterone-induced sodium transport in $mpkCCD_{cl4}$ cells. (A) The transepithelial Na^+ transport, assessed by I_{eq}, was measured on $mpkCCD_{cl4}$ cells grown on filters with or without actinomycin D (Actino., 10^{-6} M), cycloheximide (Cyclo., 0.3 μg/ml), aldosterone (Aldo., 5×10^{-7} M), Aldo. plus Actino. or Aldo. plus Cyclo. for 2 and 6 h. Values are means ± SEM from three experiments. (B) Immunoprecipitation of the α-ENaC subunit from cells labeled with [^{35}S]methionine (30 min) after incubation for 2 h (top panel) and 6 h (bottom panel). Lanes 1, untreated cells; lanes 2, actinomycin D-treated cells; lanes 3, aldosterone-treated cells; lanes 4, aldosterone plus actinomycin D-treated cells.

Discussion

An Ex Vivo Model of CCD Principal Cells

The $mpkCCD_{cl4}$ cell clone has the phenotype of a polarized tight epithelium with morphologic and functional features retained from the parental principal CCD cells. Previously characterized SV40-transformed rat rCCD1 cells (15), and the immortalized mouse M-1 CCD cells (13) both contain the two main CCD cell types, principal (PC) and intercalated (IC) cells. $mpkCCD_{cl4}$ cells are essentially PC, since they respond to vasopressin, and more than 90% of the cells do not bind DBA. IC are primarily involved in acid/base secretion, whereas PC are the main cells implicated in sodium absorption and potassium secretion in the rat and rabbit (46). In accordance with the presence of a significant Ba^{2+}-sensitive K^+ conductance in the basolateral membrane of the rat CCD (47), Ba^{2+} (10^{-4} M) added to the basal side of the $mpkCCD_{cl4}$ cells inhibits I_{sc} by almost 20%, but has no effect when added apically (data not shown). However, we did not check the ability of the cells to secrete potassium. The results from short-circuit current experiments performed with aldosterone and corticosterone, together with the identification of the CCD-specific 11β-HSD2 isoform (25,31), indicate that these clonal mouse principal CCD cells display all of the features of *bona fide* electrogenic amiloride-sensitive sodium transport stimulated by aldosterone.

Several groups have attempted to establish lines of collecting duct cells, but most, if not all of them, did not maintain the steroid hormonal control of ionic transport. Although aldosterone has been shown to increase I_{sc} in one subclone of MDCK cells (48), the I_{sc} values that were measured remained very low, about 100-fold lower than those of $mpkCCD_{cl4}$ cells. The M-1 cells, derived from isolated CCD from mice transgenic for the early region of SV40 (13), can still produce the ENaC subunits (49), but are insensitive to aldosterone (B. C. Rossier, personal communication). Because the M-1 and our mpkCCD cells are both derived from transgenic mice harboring the large T antigen, this difference is not readily explained. One possible explanation is that we used a transgene in which the immortalizing SV40 large T antigen is under the control of the L-PK tissue-specific promoter. The L-PK gene is a particular example of a gene controlled by the combination of two pairs of proximal-distal regions, each specific to hepatocytes, enterocytes, and proximal tubule cells, or erythroid cells (50). This gene is also regulated by diet (carbohydrate-rich diet) and hormones (51). A 183-bp proximal promoter of the L-PK gene, referred to as the L-type promoter, is all that is needed to direct tissue-specific expression in the liver, kidney, and intestine from transgenic mice (19). Miquerol *et al.* (20) have created new lines of transgenic mice to determine the influence of the distal region (−1000 to −3000 bp) of the L-PK promoter gene

on diet responsiveness and tissue specificity. They found that the expression of Tag directed by composite regulatory sequences consisting of the L-PK promoter fused to the SV40 early enhancer was regulated by a carbohydrate-rich diet. Strikingly, the expression of the transgene was considerably increased in the kidney, and particularly in CCD. This finding, in part related to the fact that the SV40 enhancer is especially strong in the kidney (52), thus permitted us to derive this new clonal mpkCCD cell line using this particular strain of transgenic mice fed a carbohydrate-rich diet.

Aldosterone-Induced Electrogenic Sodium Transport in Mouse CCD Principal Cells

Two amphibian cell lines (TBM and A6) have been the classical *ex vivo* cell model systems used to analyze the action of aldosterone on sodium transport (1). The present report shows that aldosterone increases sodium absorption in a clone of mouse CCD principal cells, mpkCCD$_{cl4,}$ within 60 to 90 min, a latent period similar to those of TBM and A6 cells. The steroid hormone progressively increases I_{sc} over 1 to 5 h, during which time the transepithelial electrical resistance decreases. Such dissociated effects of aldosterone closely resemble that described for A6 cells (2).

Aldosterone stimulates sodium channels and sodium pumps via its specific binding to corticosteroid receptors (53). Like other target tissues for aldosterone, CCD possess the two corticosteroid receptors MR and GR. The relatively high concentration of aldosterone (5×10^{-7} M) required to stimulate maximal Na^+ absorption suggests that aldosterone occupies GR. Results from RT-PCR performed with rat MR primers and digestion of the amplified products by restriction enzymes (26) strongly suggest that the mpkCCD$_{cl4}$ cells have maintained the expression of the MR gene. Binding studies also indicate that these cells have one class of high affinity receptor for aldosterone, MR, as in A6 cells and intact rabbit CCD (42,43). The binding site for [^{3}H]dexamethasone in the mpkCCD$_{cl4}$ cells has the same characteristics as GR. The glucocorticoid receptor antagonist RU486 does not prevent the rise in I_{sc} caused by 10^{-9} M aldosterone, but almost completely prevented the rise in I_{sc} caused by 5×10^{-7} M aldosterone or corticosterone. In mpkCCD$_{cl4}$ cells, in which 11β-HSD2 is fully active, corticosterone will be metabolized and not bind to either MR or GR. Under this condition, however, low concentrations of aldosterone ($\leq 10^{-9}$ M) will bind to MR, whereas higher concentrations of aldosterone ($\geq 10^{-9}$ M) will occupy GR as well. Interestingly, Geering *et al.* (54) have shown that the aldosterone-dependent sodium transport response was mediated by occupancy of both type 1 (MR) and type 2 (GR) receptors in the toad bladder system, and that at least 55% of the overall Na^+ transport response was mediated by the occupancy of GR by aldosterone. In the present study, we show that this scenario may also take place in the mpkCCD$_{cl4}$ cell line; the proportion of the sodium transport mediated by GR occupancy, however, appears to be slightly higher.

Action of Aldosterone on α-ENaC mRNA and Protein Synthesis in Mouse CCD Principal Cells

The increase in sodium permeability in aldosterone-responsive cells is due to enhanced sodium transport via the amiloride-sensitive sodium channel (1). There may be several not mutually exclusive ways of activating the sodium channel. Aldosterone may initially activate preexisting Na^+ channels (11), but this has not been unambiguously proved (55). A recent study on A6 cells demonstrated that the α-ENaC subunit has a short half-life (approximately 50 min) and that aldosterone increases the rate of α-ENaC subunit within 60 min, in parallel with the increase in I_{sc} (23). These observations raise the possibility that *de novo* synthesis of α-ENaC, which is the limiting factor in the assembly and/or export of newly synthesized ENaC to the plasma membrane (56), is part of the early effect of aldosterone on Na^+ transport. Our results show that aldosterone also increases the amounts of both α-ENaC mRNA and protein in mpkCCD$_{cl4}$ cells. The increase in α-ENaC protein synthesis is already detectable after incubation with 5×10^{-7} M aldosterone for 2 h, which correlates well with the increase in I_{sc} produced by aldosterone (Figures 7 and 10). Thus, corticosteroid hormones rapidly stimulate α-ENaC protein synthesis in these cultured mammalian CCD cells. The early (2 h) and late (6 h) increases in Na^+ transport induced by aldosterone are impaired by the transcription inhibitor actinomycin D. Actinomycin D also prevents the increase in α-ENaC protein produced by aldosterone.

Increased γ-ENaC mRNA production has been also reported in primary cultured rabbit CCD cells (57). We found that aldosterone had no significant effect on β- or γ-ENaC subunits, in agreement with findings in A6 cells (23). These apparent differences may arise because cells in primary culture have populations of both PC and IC, whereas the clonal mpkCCD$_{cl4}$ cells are essentially principal cells. Aldosterone has a clear effect on I_{sc} and on α-ENaC mRNA and protein in cultured principal mpkCCD$_{cl4}$ cells, but Renard *et al.* (58) detected no change in this channel subunit in kidneys from rats after chronic treatment with aldosterone. Asher *et al.* (59), in contrast, found that aldosterone and dexamethasone only slightly stimulated α-rENaC mRNA synthesis, but not that of β- or γ-rENaC mRNA in the rat kidney cortex. One cannot exclude that the major effect of aldosterone on α-ENaC mRNA and protein syntheses observed in cultured CCD cells is related to different or altered biosynthesis pathways compared with intact kidneys. The differences observed between intact kidney and primary cultured CCD (35), or the present mpkCCDcl4 cultured cells on the effects of aldosterone on Na transport suggest that GR remains the main steroid receptor pathway in cultured kidney CCD cells. However, a significant rise in Na transport remains detectable in the present established mouse CCD principal cell line using low concentrations of aldosterone ($\leq 10^{-8}$ M), thus suggesting that these cells have conserved functional MR receptors.

In conclusion, we have produced a new clone of mammalian principal cells that have retained their sodium transport capacities and are stimulated by corticosteroid hormones. These transimmortalized mouse CCD cells should provide a murine

cell system in which to develop a strategy for identifying corticosteroid-induced or -repressed proteins.

Acknowledgments

This study was supported by the Institut National de la Santé et de la Recherche Médicale and by grants from the Association pour la Recherche sur le Cancer (no. 6797) and the European Union (BIO 4 CT 960052). We thank D. Hanahan for the anti-Tag antibody, D. Paulin for the anti-cytokeratins K_8-K_{18} antibody, and M. Caplan for the anti-Na^+,K^+-ATPase antibody. We thank D. Martini (Hoechst Marion Roussel Laboratories), who kindly provided the RU26752. We also thank S. Roger and P. Disdier for photographic work and O. Parkes for editorial assistance.

References

1. Rossier BC, Palmer LG: Mechanisms of aldosterone action on sodium and potassium transport. In: *The Kidney: Physiology and Pathophysiology*, edited by Seldin DW, Giebisch G, New York, Raven, 1992, pp 1373–1409
2. Verrey F, Schaerer E, Zoerkler P, Paccolat MP, Geering K, Kraehenbuhl JP, Rossier BC: Regulation by aldosterone of Na^+, K^+-ATPase mRNAs, protein synthesis, and sodium transport in cultured kidney cells. *J Cell Biol* 104: 1231–1237, 1987
3. Paccolat MP, Geering K, Gaeggeler HP, Rossier BC: Aldosterone regulation of Na^+ transport and Na^+-K^+-ATPase in A6 cells: Role of growth conditions. *Am J Physiol* 252: C468–C476, 1987
4. Verrey F: Transcriptional control of sodium transport in tight epithelia by adrenal steroids. *J Membr Biol* 144: 93–110, 1995
5. Vallet V, Chraibi A, Gaeggeler HP, Horisberger JD, Rossier BC: An epithelial serine protease activates the amiloride-sensitive sodium channel. *Nature* 389: 607–610, 1997
6. Handler JS, Perkins FM, Johnson JP: Hormone effects on transport in cultured epithelia with high electrical resistance. *Am J Physiol* 240: C103–C105, 1981
7. Verrey F, Beron J, Spindler B: Corticosteroid regulation of renal Na, K-ATPase. *Miner Electrolyte Metab* 22: 279–292, 1996
8. Canessa CM, Horisberger J-D, Rossier BC: Epithelial sodium channel related to proteins involved in neurodegeneration. *Nature* 361: 467–470, 1993
9. Canessa CM, Schild L, Buell G, Thorens B, Gautschi I, Horisberger J-D, Rossier BC: Amiloride-sensitive epithelial Na^+ channel is made of three homologous subunits. *Nature* 367: 463–467, 1994
10. Palmer LG, Frindt G: Amiloride-sensitive Na channels from the apical membrane of the rat cortical collecting tubule. *Proc Natl Acad Sci USA* 83: 2767–2770, 1986
11. Kemendy AE, Kleyman TR, Eaton DC: Aldosterone alters the open probability of amiloride-blockable sodium channel in A6 epithelia. *Am J Physiol* 263: C825–C837, 1992
12. Duc C, Farman N, Canessa CM, Bonvalet JP, Rossier BC: Cell-specific expression of epithelial sodium channel α, β, γ subunits in aldosterone-responsive epithelia from the rat: Localization by in situ hybridization and immunocytochemistry. *J Cell Biol* 127: 1907–1921, 1994
13. Stoos BA, Náray-Fejes-Tóth A, Carretero OA, Ito S, Fejes-Tóth G: Characterization of a mouse cortical collecting duct cell line. *Kidney Int* 39: 1168–1175, 1991
14. Rafestin-Oblin ME, Farman N, Cassingéna R, Ronco P, Vandewalle A: Mineralocorticoid receptors in SV-40 transformed tubule cell lines derived from rabbit kidney. *J Steroid Biochem Mol Biol* 44: 45–52, 1993
15. Blot-Chabaud M, Laplace M, Cluzeaud F, Capurro C, Cassingéna R, Vandewalle A, Farman N, Bonvalet JP: Characteristics of a rat cortical collecting duct cell line that maintains high transepithelial resistance. *Kidney Int* 50: 367–376, 1996
16. Briand P, Kahn A, Vandewalle A: Targeted oncogenesis: A useful tool to derive renal epithelial cell lines. *Kidney Int* 47: 388–394, 1995
17. Cartier N, Lacave R, Vallet V, Hagege J, Hellio R, Robine S, Pringault E, Cluzeaud F, Briand P, Kahn A, Vandewalle A: Establishment of proximal tubule cell lines by targeted oncogenesis in transgenic mice using the L-pyruvate kinase-SV40 (T) antigen hybrid gene. *J Cell Sci* 104: 695–704, 1993
18. Bens M, Bogdanova A, Cluzeaud F, Miquerol L, Kerneis S, Kraehenbuhl JP, Kahn A, Pringault E, Vandewalle A: Transimmortalized mouse intestinal cells (m-IC_{cl2}) that maintain a crypt phenotype. *Am J Physiol* 270: C1666–C1674, 1996
19. Cartier N, Miquerol L, Tulliez M, Lepetit N, Levrat F, Grimber G, Briand P, Kahn A: Diet-dependent carcinogenesis of pancreatic islets and liver in transgenic mice expressing oncogenes under the control of the L-type pyruvate kinase gene promoter. *Oncogene* 7: 1413–1422, 1992
20. Miquerol L, Cluzeaud F, Porteu A, Alexandre Y, Vandewalle A, Kahn A: Tissue specificity of L-pyruvate kinase transgenes results from combinatorial effects of proximal promoter and distal activator regions. *Gene Expression* 5: 315–330, 1996
21. Duong Van Huyen JP, Bens M, Vandewalle A: Differential effects of aldosterone and vasopressin on chloride fluxes in transimmortalized mouse cortical collecting duct cells. *J Membr Biol* 164: 79–90, 1998
22. Fejes-Tóth G, Náray-Fejes-Tóth A: Isolated principal and intercalated cells: Hormone responsiveness and Na^+-K^+-ATPase activity. *Am J Physiol* 256: F742–F750, 1989
23. May A, Puoti A, Gaeggeler HP, Horisberger JD, Rossier BC: Early effect of aldosterone on the rate of synthesis of the epithelial sodium channel α subunit in A6 renal cells. *J Am Soc Nephrol* 8: 1813–1822, 1987
24. Hummler E, Barker P, Gatzy J, Beermann F, Verdumo C, Schmidt A, Boucher R, Rossier BC: Early death due to the defective neonatal lung liquid clearance in αENaC-deficient mice. *Nat Genet* 12: 325–328, 1996
25. Cole TJ: Cloning of the mouse 11 β-hydroxysteroid dehydrogenase type 2 gene: Tissue specific expression and localization in distal convoluted tubules and collecting ducts of the kidney. *Endocrinology* 136: 4693–4696, 1995
26. Todd-Turla AM, Schnermann J, Fejes-Tóth G, Náray-Fejes-Tóth A, Smart A, Killen PD, Briggs JP: Distribution of mineralocorticoid and glucocorticoid receptor mRNA along the nephron. *Am J Physiol* 264: F781–F791, 1993
27. Rafestin-Oblin ME, Couette B, Radanyi C, Lombes M, Baulieu EE: Mineralocorticosteroid receptor of the chick intestine Oligomeric structure and transformation. *J Biol Chem* 264: 9304–9309, 1989
28. Bradford MM: A rapid and sensitive method for the quantitation of microgram quantities of protein utilizing the principle of protein-dye binding. *Anal Biochem* 72: 248–254, 1976
29. Claire M, Rafestin-Oblin ME, Michaud M, Corvol P, Verrot A, Roth-Meyer C, Boisvieux JF, Mallet A: Statistical test of models and computerized parameter estimation for aldosterone binding in rat kidney. *FEBS Lett* 88: 295–299, 1978
30. Alfaidy N, Blot-Chabaud M, Bonvalet JP, Farman N: Vasopres-

sin potentiates mineralocorticoid selectivity by stimulating 11 beta hydroxysteroid dehydrogenase in rat collecting duct. *J Clin Invest* 10: 2437–2442, 1997
31. Náray-Fejes-Tóth A, Rusval E, Fejes-Tóth G: Mineralocorticoid receptors and 11 β-steroid dehydrogenase activity in renal principal and intercalated cells. *Am J Physiol* 266: F76–F80, 1994
32. Schuster VL: Function and regulation of collecting duct intercalated cells. *Annu Rev Physiol* 55: 267–288, 1993
33. Kleyman TR, Cragoe EJ: Amiloride and its analogs as tools in the study of ion transport. *J Membr Biol* 105: 1–21, 1988
34. Vigne P, Frelin C, Cragoe EJ, Ladzunski M: Ethylisopropylamiloride: A new and highly potent derivative of amiloride for the inhibition of the Na^+/H^+ exchange system in various cell types. *Biochem Biophys Res Commun* 116: 86–90, 1983
35. Náray-Fejes-Tóth A, Fejes-Tóth G: Glucocorticoid receptors mediate mineralocorticoid-like effects in cultured collecting duct cells. *Am J Physiol* 259: F672–F678, 1990
36. Duncan RI, Grogan WM, Kramer LB, Watlington CO: Corticosterone's metabolite is an agonist for Na^+ transport stimulation in A6 cells. *Am J Physiol* 255: F736–F748, 1988
37. Schmidt TJ, Husted RF, Stokes JB: Steroid hormone stimulation of Na^+ transport in A6 cells is mediated via glucocorticoid receptors. *Am J Physiol* 264: C875–C884, 1993
38. Monder C, Stewart PM, Lakshmi V, Valentino R, Burt D, Edwards CR: Licorice inhibits corticosteroid 11 β-dehydrogenase of rat kidney and liver: In vivo and in vitro studies. *Endocrinology* 125: 1046–1053, 1989
39. Gaeggeler HP, Duperrex H, Hautier S, Rossier BC: Corticosterone induces 11 β-HSD and mineralocorticoid specificity in an amphibian urinary bladder cell line. *Am J Physiol* 264: C317–C322, 1993
40. Edwards CRW, Stewart PM, Burt D, Brett L, McIntyre MA, Sutano WS, de Kloet ER, Monder C: Localization of 11β-hydroxysteroid dehydrogenase-tissue specific protector of the mineralocorticoid receptor. *Lancet* 2: 986–989, 1988
41. Funder JW, Pearce PT, Smith R, Smith AI: Mineralocorticoid action: Target tissue specificity is enzyme, not receptor, mediated. *Science* 242: 583–585, 1988
42. Farman N, Vandewalle A, Bonvalet JP: Aldosterone binding in isolated tubule. I. Biochemical determination in proximal and distal parts of the rabbit nephron. *Am J Physiol* 242: F63–F68, 1982
43. Claire M, Machard B, Lombes M, Oblin ME, Bonvalet JP: Aldosterone receptors in A6 cells: Physicochemical characterization and autoradiographic study. *Am J Physiol* 257: C665–C677, 1989
44. Perroteau I, Netchitailo P, Delarue C, Leboulenger F, Philibert D, Deraedt R, Vaudry H: The effect of the antimineralocorticoid RU 28318 on aldosterone biosynthesis in vitro. *J Steroid Biochem* 20: 853–856, 1984
45. Ulmann A, Bertagna C, Le Go A, Husson JM, Tache A, Sassano P, Menard J, Corvol P: Assessment of the antimineralocorticoid effect of RU 28318 in healthy men with induced exogenous and endogenous hypermineralocorticism. *Eur J Pharmacol* 28: 531–535, 1985
46. Stanton BA, Giebisch G: *Handbook of Physiology-Renal Physiology*, edited by Windhager E, Oxford, Oxford University Press, 1992, pp 813–874
47. Schlatter E, Lohrmann E, Greger G: Properties of the potassium conductance of principal cells of rat cortical collecting ducts. *Pflügers Arch* 420: 39–45, 1992
48. Blazer-Yost BL, Record RD, Oberleithner H: Characterization of hormone-stimulated Na^+ transport in a high-resistance clone of the MDCK cell line. *Pflügers Arch* 432: 685–691, 1996
49. Letz B, Ackermann A, Canessa CM, Rossier BC, Korbmacher C: Amiloride-sensitive channels in confluent M-1 mouse cortical collecting duct cells. *J Membr Biol* 148: 127–141, 1995
50. Noguchi T, Yamada K, Inoue H, Matsuda T, Tanaka T: The L- and R-type isoforms of rat pyruvate kinase are produced from a single gene by use of different promoters. *J Biol Chem* 262: 14366–14371, 1987
51. Bergot M-O, Diaz-Guerra M-JM, Puzenat N, Raymondjean M, Kahn A: Cis-regulation of the L-type pyruvate kinase gene promoter by glucose, insulin and cyclic AMP. *Nucleic Acids Res* 20: 1871–1878, 1992
52. Feigenbaum L, Hinrichs SH, Jay G: JC virus and simian virus 40 enhancers and transforming proteins: Role in determining tissue specificity and pathogenicity in transgenic mice. *J Virol* 66: 1176–1182, 1992
53. Verrey F, Beron J: Activation and supply of channels and pumps by aldosterone. *New Physiol Sci* 11: 126–133, 1996
54. Geering K, Claire M, Gaeggeler HP, Rossier BC: Receptor occupancy vs. induction of Na^+-K^+-ATPase and Na^+ transport by aldosterone. *Am J Physiol* 248: C102–C108, 1985
55. Pacha J, Frindt G, Antonian L, Silver RB, Palmer LG: Regulation of Na channels of the rat cortical collecting tubule by aldosterone. *J Gen Physiol* 102: 25–42, 1993
56. Firsov D, Schild L, Gautschi I, Mérillat AM, Schneeberger E, Rossier BC: Cell surface expression of the epithelial Na channel and a mutant causing Liddle syndrome: A quantitative approach. *Proc Natl Acad Sci USA* 93: 15370–15375, 1996
57. Denault DL, Fejes-Tóth G, Náray-Fejes-Tóth A: Aldosterone regulation of sodium channel γ-subunit mRNA in cortical collecting duct cells. *Am J Physiol* 271: C423–C428, 1996
58. Renard S, Voilley N, Bassilana F, Ladzunski M, Barbry P: Localization and regulation by steroids of the α, β, and γ subunits of the amiloride-sensitive Na^+ channel in colon, lung and kidney. *Pflügers Arch* 430: 299–307, 1995
59. Asher C, Wald H, Rossier BC, Garty H: Aldosterone-induced increase in the abundance of Na^+ channels subunits. *Am J Physiol* 271: C605–C611, 1996